NACA TN 3591

# NATIONAL ADVISORY COMMITTEE FOR AERONAUTICS

TECHNICAL NOTE 3591

INVESTIGATION OF FAR NOISE FIELD OF JETS

II - COMPARISON OF AIR JETS AND JET ENGINES

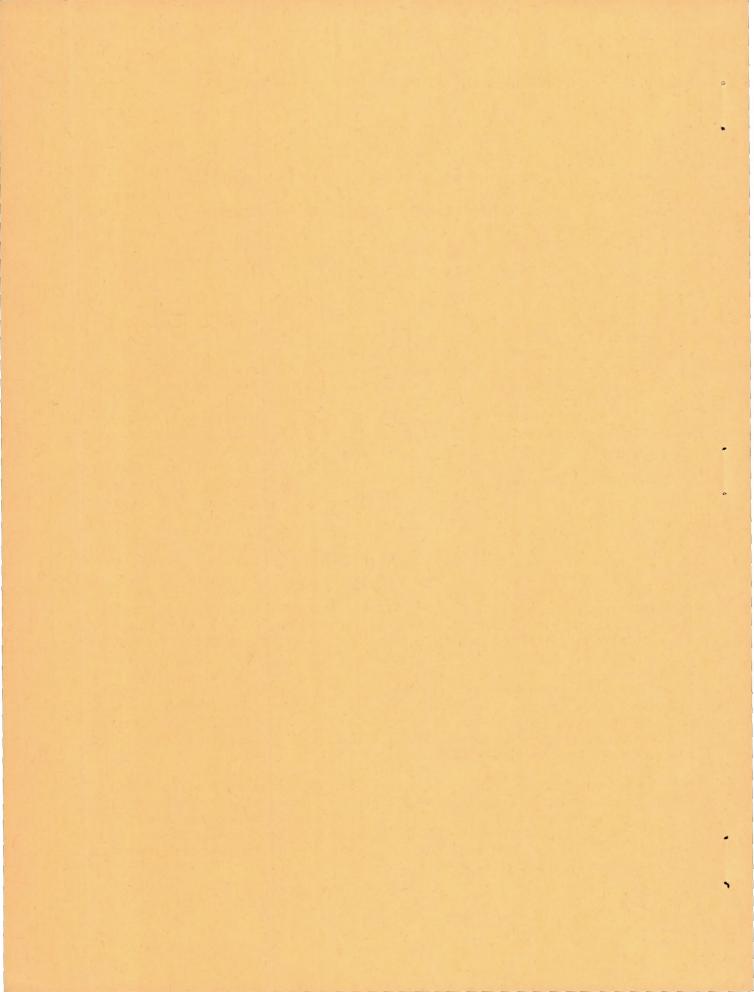
By Willard D. Coles and Edmund E. Callaghan

Lewis Flight Propulsion Laboratory Cleveland, Ohio



Washington

January 1956



43.N21/5:6/3591/errata

#### ERRATA

NACA TN 3591

INVESTIGATION OF FAR NOISE FIELD OF JETS II - COMPARISON OF AIR JETS AND JET ENGINES By Willard D. Coles and Edmund E. Callaghan

January 1956

Page 19, figure 11: The abscissa scale should read .01, .02, .04, .06, .08, .1, .2, .4, .6, .8, 1, 2, 4, 6, 8, 10, 20.

#### TECHNICAL NOTE 3591

INVESTIGATION OF FAR NOISE FIELD OF JETS

II - COMPARISON OF AIR JETS AND JET ENGINES

By Willard D. Coles and Edmund E. Callaghan

#### SUMMARY

A comparison of the noise generation of air jets and turbojet engines has been made from data obtained under similar free-field conditions. At jet pressure ratios below or only slightly above that for choked flow, the over-all sound power is well represented by the Lighthill parameter, but the results obtained with the afterburning data are somewhat low. Application of a correction to the directional data using nozzle-area ratio and jet velocity ratio to the 8<sup>th</sup> power gave good correlation between air-jet and engine data. Air-jet and engine spectral data were dissimilar because of a dip in the engine noise spectrum, which was probably caused by a combination of ground-reflection effects and additions to portions of the spectrum by compressor and combustion noise.

# INTRODUCTION

Noise emanating from air jets and jet engines has been the subject of considerable study in the United States and Great Britain. Greatly increased jet-engine size and usage combined with the promise of even larger, more powerful engines in increasing numbers make the noise problem extremely formidable. Experimental investigations with air jets (refs. 1 to 3) have shown good agreement with results predicted by Lighthill from a theoretical treatment on sound generated aerodynamically (ref. 4). Reference 1 correlated data from air-jet and jet-engine studies, some of which were free-field, test cell, and reverbrant and anechoic chamber data. As part of the general investigation conducted at the NACA Lewis laboratory of the far noise field of jets, the results presented in this report provide a comparison between air-jet and engine data measured under similar free-field conditions.

Data showing the noise characteristics of convergent, circular airjet nozzles and the correlation of the noise characteristics with jet size are presented in reference 3. Because the sound-power and spectra data presented in reference 3 show the effect of nozzle size to be a direct relation, only the data for the 4-inch-diameter nozzle are presented for the most part in this report.

The variation of the noise parameter for a wide range of jet pressure ratios (jet total pressure/atmospheric pressure) is also included in reference 3. The air-jet results presented herein are limited to jet pressure ratios in the range of the engines investigated. For purposes of comparison with engine data, the results obtained at pressure ratios near choking are of most interest. The sound fields, spectra, and sound power of these air jets are compared to corresponding characteristics of two jet engines. The engines were of the axial-flow type, the larger having approximately twice the thrust of the smaller engine. A limited amount of data was also obtained with both engines using afterburners.

In determining the characteristics of a noise source, no aspects of human response to the noise are considered. Reference 5 presents methods of determining human reaction to sounds of different levels and frequencies and also gives a comprehensive bibliography on the subject.

#### APPARATUS AND PROCEDURE

#### Air Jet

Schematic elevation and plan views of the air-jet facility are shown in figure 1. The air heater, throttling valve, flow-measurement orifice, mufflers, plenum tank, and inlet diffuser section are indicated. Screens were used inside the diffuser section to provide uniform velocity at the bellmouth entry to the nozzles. Additional description of the equipment is given in reference 3. Compressed air was supplied from remotely located compressors so that no problem of compressor-noise elimination existed.

The sound survey field indicating the relative positions of nearby buildings is shown in figure l(b). The sound measurement stations are shown on the three concentric sectors of circles with origins at the nozzle exit. The 15 measurement stations on each arc are in  $15^{\rm O}$  increments and extend from  $120^{\rm O}$  from the jet direction on one side to  $90^{\rm O}$  from the jet direction on the other.

Three  $60^{\circ}$ -convergent nozzles of 3- to 5-inch throat diameter were used. A photograph showing one of the nozzles, the plenum tank, and nearby piping is shown in figure 2.

# Turbojet Engines

The turbojet engines used in the investigation were of the axial-flow type and had rated sea-level thrust values of 5000 and 10,000 pounds. Under rated conditions, the total- to static-pressure ratio across the exhaust nozzle was 1.7 for the smaller engine (engine A) and approximately 2.2 for the larger engine (engine B). Each of the engines was mounted in the thrust stand, shown with engine B in figure 3. The engines were

NACA TN 3591 3

equipped with large inlet bellmouth sections, and on engine B a screen was provided at the bellmouth entrance to prevent ingestion of foreign material.

In addition to thrust measurements, fuel and air flows through the engine and jet temperature were measured in order to check engine performance and determine jet velocity, which is of prime importance in the aerodynamic generation of sound.

Figure 4 shows the plan view of the engine sound field. The sound measurements were taken 4 to 5 feet above ground level in 15° increments over the three quadrants. Sound measurements for engine A were taken at both 100- and 200-foot radii from the engine, and for engine B at the 200-foot radius. The control room was located about 100 feet from the engine in the quadrant in which no sound measurements were taken and, because of its small size and location, had negligible sound-reflection effects. The nearest large reflecting surface forward of the engine was approximately 600 feet away, and the sound field to the rear and sides was unobstructed for over 1/2 mile.

#### Acoustic Measurements

For purposes of standardization of nomenclature, the acoustic terms used herein are those defined in reference 6. Sound-pressure-level measurements were made with a commercial sound-level meter. Measurements were usually taken at each of the sound measurement stations at one or more radial distances for the air jet (fig. 1(b)) and the engines (fig. 4). Frequency spectra were measured when the over-all field survey was made, but at 1 radial distance (200-ft rad, nonafterburning engine; 400-ft rad, afterburning engine; and 50-ft rad, air jet). Some spectrum data were obtained at all azimuths for engine B and the air jet, and at azimuths of 30°, 90°, and 180° from the jet direction for engine A. The frequency distributions were measured with an automatic audio-frequency analyzer and recorder. Before each test, both the sound-level meter and frequency recorder were calibrated with a small loudspeaker-type calibrator and transistor oscillator. The frequency analyzer was mounted in an acoustically insulated truck, and direct field records were obtained.

For operation of the air-jet facility, the sound-pressure and spectra data were recorded at up to 15 values of total- to static-pressure ratio across the nozzle in ascending order of pressure ratio. The air was heated to approximately 200° F to eliminate condensation phenomena in the jet.

 $<sup>^{1}</sup>$ Sound-pressure level in decibels is based on a reference of 0.0002 dyne/cm $^{2}$ .

The engine-noise data of primary importance corresponds to take-off and initial climb conditions. Therefore, most of the data are for full-engine-power condition.

The sound power radiated from a jet source can be calculated by an integration process from the sound-pressure-level measurements by the method described in references 6 and 7. The same procedure is applied to the sound-pressure levels obtained for each 1/3-octave band of frequencies from the frequency-analyzer data to give the frequency distribution of the sound power. Sound-power level is based on a reference of  $10^{-13}$  watts.

#### RESULTS AND DISCUSSION

The far-field noise characteristics of a source can be completely defined when the directional distribution, frequency spectrum, and sound power of the source are known. However, differences in data are obtained because of technique and instrumentation variations.

In the following sections, data for both air jets and engines as a sound source are presented and compared in the following order: directional distribution, sound power, and frequency spectrum.

#### Air Jets

The directional characteristics of the noise from the 4-inch-diameter air jet are shown in figure 5 for two values of jet pressure ratio for three 1/3-octave frequency bands and the over-all frequency range. The directional distribution is symmetrical about the jet axis, and therefore only one side is presented. For frequency values up to and including 1000 cps, a pronounced lobe of higher sound-pressure level exists near the 30° azimuth from the jet direction. For frequencies above 1000 cps, the sound field is more nearly nondirectional. The over-all data (all frequencies) show the lobe at 30° with a relatively smooth, nearly circular pattern elsewhere.

#### Engines

The complexity of the noise from a turbojet engine is illustrated by the directional distribution of the sound for engine B with no after-burning at 100- and 80-percent rated thrust (figs. 6(a) and (b), respectively) and with afterburning (fig. 6(c)). The prominent lobed regions centered between the  $30^{\circ}$  and  $60^{\circ}$  azimuths from the jet direction emphasize the considerable reduction in level at all frequencies in the direction directly behind the jet and to a  $15^{\circ}$  azimuth. In addition,

3845

relatively strong lobes are evident in the forward quadrant for many of the frequency bands. This is especially true of the 1000-cps data at rated engine thrust. This increase in the high-frequency noise forward of the engine is undoubtedly due to compressor noise.

# Air-Jet and Engine Comparison

Because of the large differences in sound power issuing from air jets and jet engines, the air-jet data are usually obtained closer to the jet, making it necessary to apply a distance correction to the data. In addition, the frequency of the sound is a function of jet diameter, and the sound power is a function of jet area and velocity.

The theoretical treatment by Lighthill (ref. 4) predicts that the noise generated aerodynamically by a jet will be proportional to the Lighthill parameter

$$\rho_0 AV^8/a_0^5$$

where

ρ<sub>0</sub> ambient air density, slugs/cu ft

A nozzle-exit area, sq ft

V jet velocity, ft/sec

an ambient acoustic velocity, ft/sec

Figure 7 shows the total sound power in kilowatts for both the air jet and engines as a function of the Lighthill parameter. The engine data are presented with and without afterburning for three values of thrust for each engine. Air-jet data for three nozzle sizes at pressure ratios below that for choked flow are also included on the figure. The line on figure 7 represents the best line through the data excluding the afterburning data. The fact that the slope of the line is exactly unity shows that, although the engine jet temperature is high and the flow slightly supersonic for the high-thrust condition of engine B, the sound power is well represented by the Lighthill parameter.

This correlation shows that, basically, the noise generated by a full-scale engine is governed by the same law as the noise of a simple air jet. Hence, it may be concluded that the principal contribution to jet-engine noise arises from the turbulent mixing of the jet with the surrounding atmosphere.

3845

NACA TN 3591

The afterburner data for both engines fall somewhat below the straight-line relation indicated for the other data. There are two probable explanations for this effect: (1) The high-temperature afterburning condition is beyond the limits of applicability of the Lighthill parameter, without considering jet density; or (2) the sound pressures generated by an afterburning jet may be of such large magnitude that the radiated sound waves are no longer of small amplitude and hence would be subject to the large attenuation effects associated with finite waves (ref. 8).

Polar diagrams of the corrected over-all directional distribution of the 4-inch-diameter air jet and two engines are shown in figure 8. The comparison shows the sound patterns to be similar with the exception of the low-noise-level region displayed by both jet engines near the jet axis. This probably results from the refractive effect on the sound in passing from the jet to the surrounding atmosphere, in which the speed of sound is lower.

Spectrum measurements made at each station around the engine and air jet are integrated as previously described, and the results are shown in figure 9. In figure 9(a) the corrected spectrum power level is presented for two pressure ratios for the 4-inch-diameter air jet. The application of the velocity-ratio correction to the choked-flow conditions (pressure ratio, 2.55) is probably not entirely valid. However, by applying this correction, the change in the spectrum resulting from the change in noise-generating mechanism due to shocked flow can be seen. An increase in the high-frequency noise is evident from the figure, and the tendency toward the formation of large-amplitude discrete frequencies is indicated. The velocity used for the choked-flow condition corresponds to full adiabatic expansion of the jet calculated from the pressure and temperature conditions at the plenum. At low frequencies the microphone is susceptible to wind noise (see ref. 3), which shows up especially in air-jet data because of the lesser magnitude of the sound power in the low frequencies.

Noise data for engine B obtained at two values of engine thrust are shown in figure 9(b). Here as with the air jet an increase in high-frequency noise occurs at the increased power condition. The minimum near the center of the curves possibly results from ground interference or reflection effects (see ref. 9). Unpublished data studied concerning this effect indicate that perhaps the phenomenon may be a function of height of the engine exhaust above ground level, thus supporting the reflectivity hypothesis.

Spectrum-level distributions for four azimuths are shown in figure 10(a). The secondary peak in the power-spectrum distributions of figure 9(b) at approximately 1000 cps also appears in all the spectra of figure 10(a), except for the 180° azimuth. The 1000-cps data of figure 6 also show this reduction in front of the engine (180° azimuth).

NACA TN 3591 7

The spectrum-level distribution during afterburner operation is shown in figure 10(b) for four azimuths. The characteristic dip in the spectra at 400 cps and the peak at 1000 cps are again evident. Spectra for the  $120^{\circ}$  azimuth were obtained but were not included because of their similarity to the  $90^{\circ}$ -azimuth data.

A comparison of the relative frequency distribution of the sound power for the air jet and engine is shown in figure 11. Cumulative sound power (percent of total sound power below a given abscissa value) is presented against Strouhal number (a dimensionless parameter). Strouhal number (frequency times diameter divided by jet velocity) is used as the abscissa to bring the curves closer together to facilitate comparison. The minimum in figure 9(b) for the engine data is shown in figure 11 by the change in slope in the middle-frequency range. The ground-reflection effect previously mentioned and the addition to the higher frequencies as a result of compressor noise probably are the reasons for the deviation from the distribution curves exhibited by the air jet. Combustion noise may also contribute to this deviation.

#### SUMMARY OF RESULTS

As part of the general program to investigate jet noise and means for its suppression, a comparison was made of the noise characteristics of air jets and turbojet engines. The following results were obtained:

- 1. The over-all sound power generated by an air jet and nonafter-burning jet engine during ground operation at pressure ratios below or only slightly above that for choked flow was correlated by the Lighthill noise-generation parameter. This result shows that the principal contribution to jet-engine noise arose from the turbulent mixing of the jet with the surrounding atmosphere.
- 2. The sound power radiated during afterburner operation of the engines was lower than indicated by the Lighthill parameter.
- 3. Correction of sound-pressure-level directional data by the nozzle-area ratio and 8<sup>th</sup> power of the velocity ratio gave good correlation of air-jet with engine data.
- 4. The spectral distribution of sound power for the engine was characterized by a dip in the middle frequencies, possibly resulting from a combination of ground-reflection effects and additions to portions of the spectrum by compressor and combustion noise. Air-jet and engine spectra showed dissimilarity due to the dip in the frequency distribution for the engine.

Lewis Flight Propulsion Laboratory
National Advisory Committee for Aeronautics
Cleveland, Ohio, October 19, 1955

# 3845

### REFERENCES

- 1. Tyler, John M., and Perry, Edward C.: Jet Noise. Preprint No. 287, SAE, 1954.
- 2. Westley, R., and Lilley, G. M.: An Investigation of the Noise Field from a Small Jet and Methods for Its Reduction. Rep. No. 53, The College of Aero. (Cranfield), Jan. 1952.
- Callaghan, Edmund E., and Coles, Willard D.: Investigation of Far Noise Field of Jets. I - Effect of Nozzle Shape. NACA TN 3590, 1955.
- 4. Lighthill, M. J.: On Sound Generated Aerodynamically. I. General. Theory. Proc. Roy. Soc. (London), ser. A., vol. 211, no. 1107, Mar. 20, 1952, pp. 564-587.
- 5. Rosenblith, Walter A., et al.: Handbook of Acoustic Noise Control.
  Vol II. Noise and Man. WADC Tech. Rep. 52-204, Aero. Medical Lab.,
  Wright Air Dev. Center, Wright-Patterson Air Force Base, June 1953.
  (Contract No. AF 33(038)-20572, RDO No. 695-63.)
- 6. Bolt, R. H., Lukasik, S. J., Nolle, A. W., and Frost, A. D., eds.:
  Handbook of Acoustic Noise Control. Vol. 1. Physical Acoustics.
  WADC Tech. Rep. 52-204, Aero. Medical Lab., Wright Air Dev. Center,
  Wright-Patterson Air Force Base, Dec. 1952. (Contract No. AF 33(038)20572, RDO No. 695-63.)
- 7. Callaghan, Edmund E., and Coles, Willard D.: Investigation of Jet-Engine Noise Reduction by Screens Located Transversely Across the Jet. NACA TN 3452, 1955.
- 8. Fay, R. C.: Plane Sound Waves of Finite Amplitude. Jour. Acous. Soc. Am., vol. 3, Oct. 1931, pp. 222-241.
- 9. Franken, Peter A.: The Field of a Random Noise Source Above an Infinite Plane. Theoretical Analysis. Acoustics Lab., M.I.T., Jan. 11, 1955.

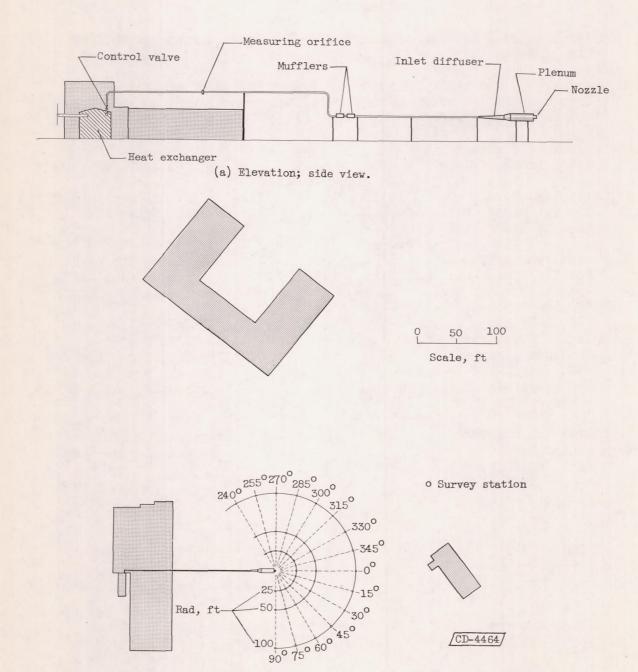


Figure 1. - Schematic diagram of air system and adjacent buildings.

(b) Plan view.

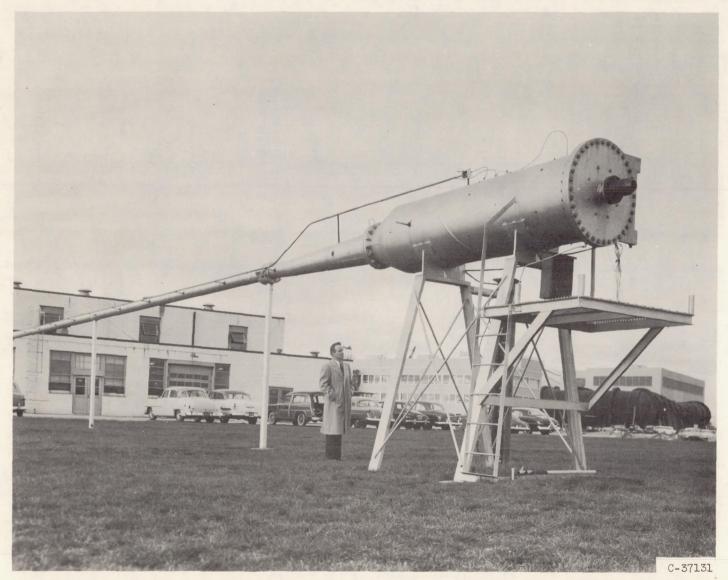


Figure 2. - Photograph of nozzle, plenum chamber, and associated piping.

Figure 3. - Thrust stand with engine B installed.

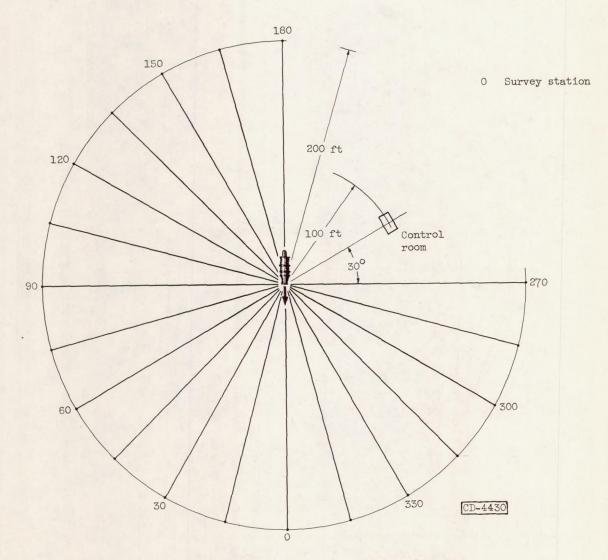


Figure 4. - Location of engine sound survey stations and control room.

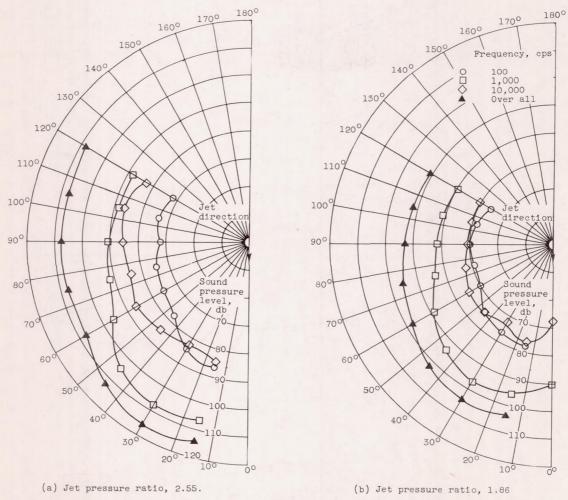


Figure 5. - Directional distribution of noise from 4-inch-diameter air jet. Distance from jet exit, 50 feet.

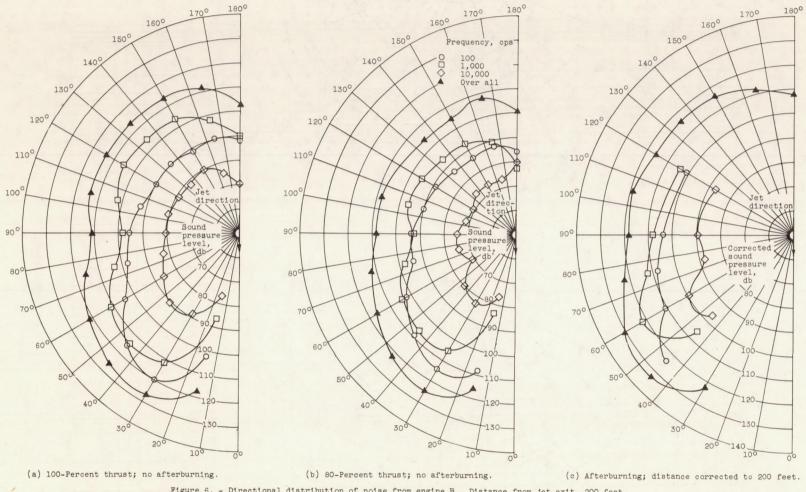


Figure 6. - Directional distribution of noise from engine B. Distance from jet exit, 200 feet.

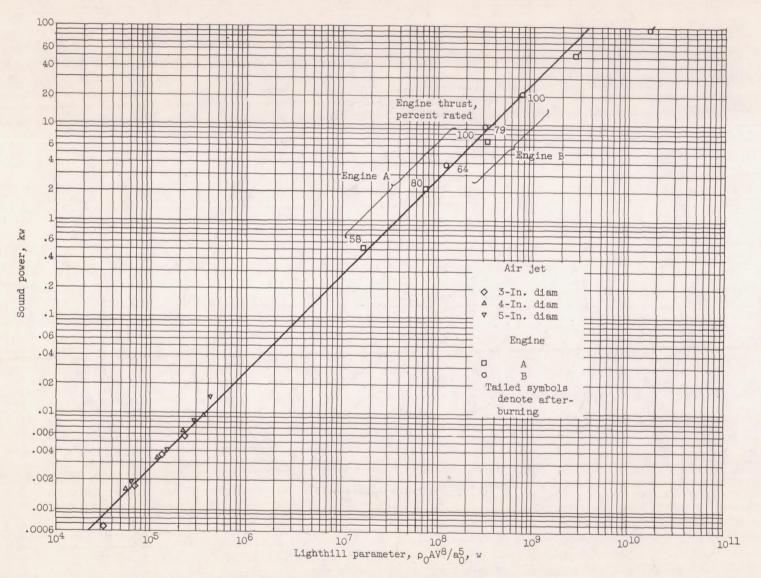


Figure 7. - Sound power as function of Lighthill parameter.

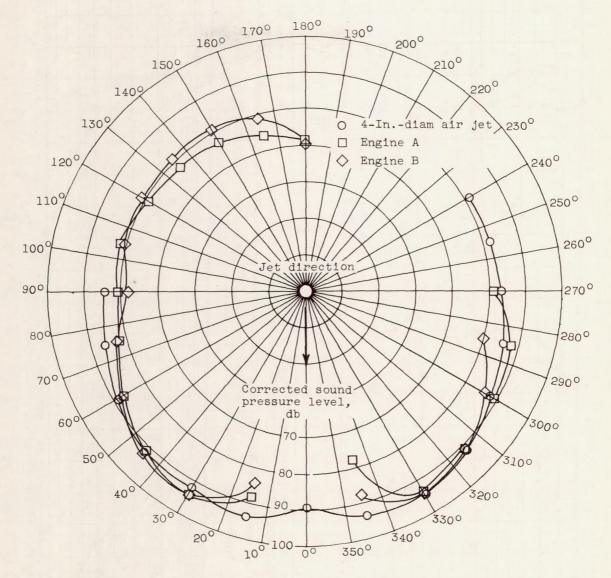


Figure 8. - Comparison of directional distribution of sound from air jet and engines. Area ratio and velocity ratio to 8<sup>th</sup>-power corrections based on air jet have been applied. Distance from jet exit, corrected to 200 feet.

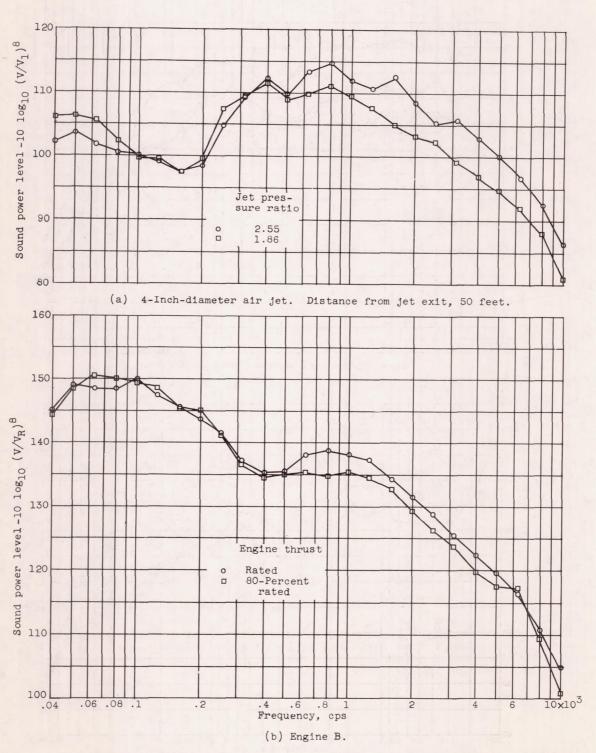


Figure 9. - Corrected spectrum power level as function of frequency.

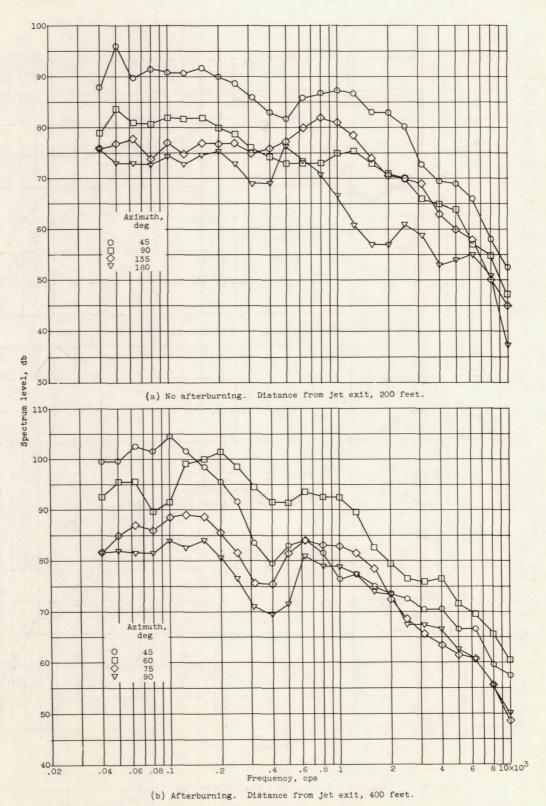


Figure 10. - Spectral distribution of noise from engine B at several azimuths.

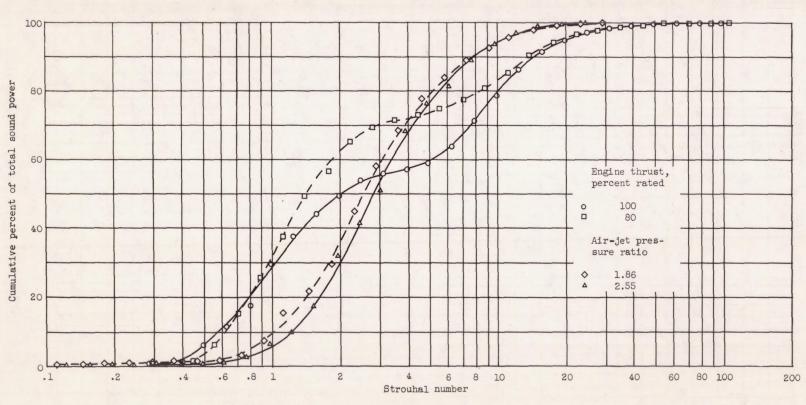


Figure 11. - Cumulative spectral distribution of sound power.

